THE JOURNAL OF PHYSICAL CHEMISTRY LETTERS
A JOURNAL OF THE AMERICAN CHEMICAL SOCIETY

pubs.acs.org/JPCL

Letter

Pseudo-Anomalous Size-Dependent Electron−Phonon Interaction in Graded Energy Band: Solving the Fano Paradox

Manushree Tanwar, Devesh K. Pathak, Anjali Chaudhary, Alexander S. Krylov, Herbert Pfnür, Ashutosh Sharma,* Byungmin Ahn,* Sangyeob Lee,* and Rajesh Kumar*

Cite This: *J. Phys. Chem. Lett.* 2021, 12, 2044−2051

Read Online

ACCESS | Metrics & More | Article Recommendations | Supporting Information

ABSTRACT: Quantum size effects on interferons (electron−phonon bound states), confined in fractal silicon (Si) nanostructures (NSs), have been studied by using Raman spectromicroscopy. A paradoxical size dependence of Fano parameters, estimated from Raman spectra, has been observed as a consequence of longitudinal variation of nanocrystallite size along the Si wires leading to local variations in the dopants' density which actually starts governing the Fano coupling, thus liberating the interferons to exhibit the typical quantum size effect. These interferons are more dominated by the effective reduction in dopants' density rather than the quantum confinement effect. Detailed experimental and theoretical Raman line shape analyses have been performed to solve the paradox by establishing that the increasing size effect actually is accompanied by receding Fano coupling due to the weakened electronic continuum. The latter has been validated by observing a consequent variation in the Raman signal from dopants which was found to be consistent with the above conclusion.

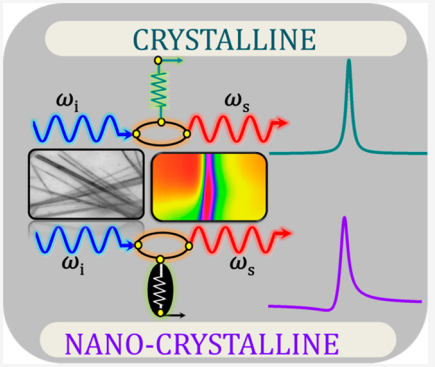

In the era of nanoscience and nanotechnology[1−10] it is difficult to be sure about how much quantum phenomena are yet to be explored.[11,12] Any novel quantum effect[13,14] astonishes one only until another newer dimension of understanding gets unfolded even in simplest forms of nanostructures (e.g., silicon) if observed and appreciated minutely. New physical insights into nanomaterials and newer challenges continue to fascinate the scientists with the latter working as the driving force too for continuing research to unveil subtler dimensions of the nanoscience and nanotechnology. Technologically important nanomaterials are equally important from the scientific point of view as these quantum structures make a good system to understand different physical phenomena and their interplays.[15−18] Numerous size-dependent variations in materials' properties either start happening (e.g., quantum confinement) or change by orders of magnitude (e.g., electron−phonon interaction, optical properties, etc.)[1,19,20] when their sizes approach the nano regime, whose onset is specific to a material and can be quantified.[11,21−23] Depending on the nature of different physical processes, the known (and understood) size-dependent properties' variation may either be or appear quite anomalous especially when more than one quantum phenomenon, specific to the nano regime, is present. These anomalies must be deconvoluted to either establish the true size dependence or understand their interrelation. Such scientific explorations must be carried in parallel with the technological advances to maintain the overall growth trajectory.[24]

At the nano scale, Fano[25−28] (or electron−phonon) interaction is also size-dependent like other properties (electrical, electronic, optical, etc.),[29−32] showing increasing coupling strength with decreasing size.[33−36] In general, the Fano interaction is a result of continuum−discrete interference where the continuum and discrete states, taking part in interference, may originate from different system specific stimuli. Raman scattering[37,38] proves to be one of the simplest experimental ways to identify the presence of Fano interaction (between discrete phonon and continuum electronic states) in terms of a typical asymmetric Raman line shape.[39] Along with Raman spectral asymmetry and the presence of antiresonance minima, the dopant concentration and dopant-type dependence of Fano parameters validate the presence of the Fano interaction in heavily doped semiconductor systems.[33,40−46] The above-mentioned straightforward observation, when takes place in semiconductor nanostructures, may yield a Raman line shape where asymmetry and antiresonance show doping and a size dependence that may look completely different from their bulk counterparts. The level of possible complications involved in the resultant Raman line shape makes it an interesting as well as challenging problem to understand the overall size

Received: January 21, 2021
Accepted: February 9, 2021
Published: February 19, 2021

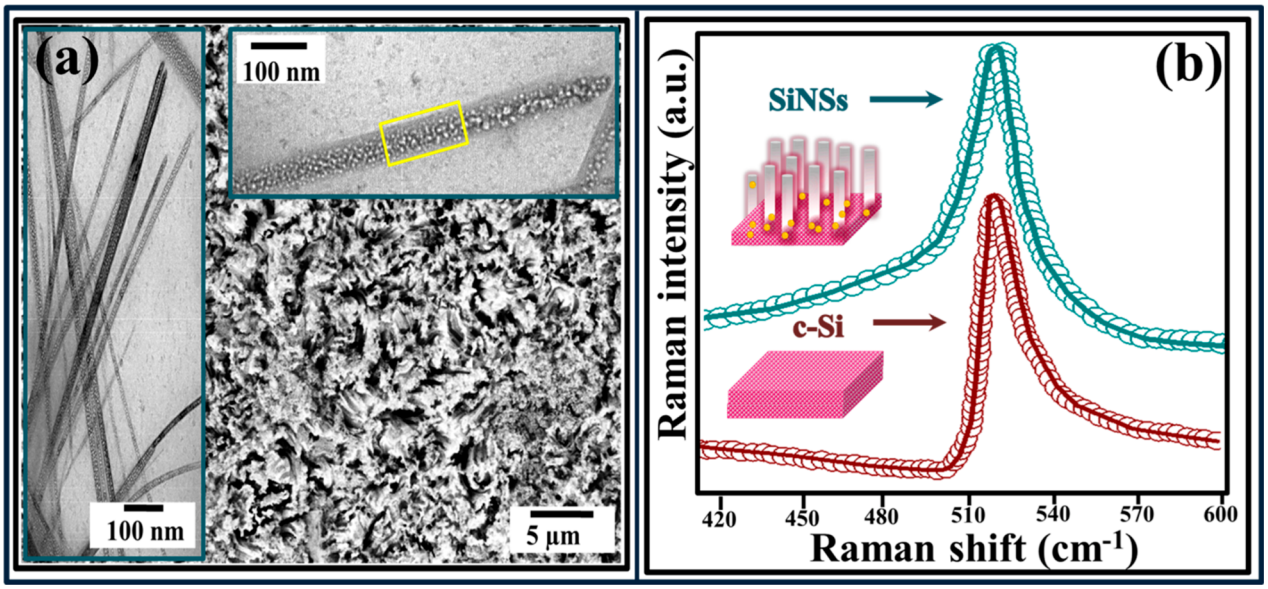

Figure 1. (a) Surface morphology of a porosified p-type Si wafer along with corresponding TEM images showing nanowires (left inset) and magnified view showing fractal structures (top right inset). (b) Raman spectra from the crystalline Si (c-Si) and Si NSs with discrete points showing the experimental data and solid lines representing the theoretical fit using the confinement model (eq 1).

dependence of a Raman line shape which is supposed to be an amalgam of various size-, doping-, and dopant-dependent contributions. This will certainly help in designing appropriate futuristic material paradigms.

The current work reports an atypical size dependence of Raman−Fano parameters from boron-doped (p-type) silicon (Si) nanostructures (NSs) up to a point where one gets deceived of observing (pseudo-)anomalous behavior. An increasing Fano coupling parameter (with decreasing size), obtained by using Fano line shape fitting of Raman spectra, is noticed which actually was found to be consistent with the known size-dependent Fano effect as established by careful deconvolution of the Raman line shape by incorporating the effect of gradual nanosize variation along the Si microwires. The wire-like structures, prepared by using metal-assisted etching, exhibit depletion of dopants as a consequence of the fabrication process[47−49] due to the fractal nature of the Si NSs. The quantum effect was found to exhibit a dual role of a typical band gap enhancement and atypical zonal dopant depletion with the latter being dominating. These two effects force the interferons to behave in a pseudo-anomalous manner only to get revealed after careful Raman line shape analysis followed by experimental validation using quantitative Raman spectromicroscopy. The gradual size variation in the prepared fractal Si NSs leads to a graded energy band system where the doping concentration also decreases inherently with decreasing size due to Fermi surface migration of dopants thus responsible for the above-stated quantum Fano effect.

A fractal structured porous Si sample consisting of Si NSs has been synthesized from a commercially available (Vin Karola) p-type Si wafer (boron-doped $\sim 10^{20}$ cm^{-3}) by metal-induced etching (MIE).[50−55] For MIE, first Ag nanoparticles (AgNPs) were deposited on cleaned Si wafers by dipping them into a solution containing 4.8 M HF and 5 mM $AgNO_3$ for 60 s at room temperature. The AgNPs (~100 nm)[56] deposited samples were then kept in an etching solution (4.6 M HF + 0.5 M H_2O_2) for 60 min at room temperature. A Supra 55 Zeiss scanning electron microscope (SEM) was used to study the surface morphologies, and Raman spectra were recorded by using a Horiba Jobin Yvon micro-Raman spectrometer with a 633 nm excitation laser with minimum power to avoid any laser-induced heating as confirmed by Stokes/anti-Stokes measurements shown in Figure S1 of the Supporting Information. Transmission electron microscopy (TEM) was performed by using a Gatan model 636MA electron microscope.

The Si wafer etched by using MIE becomes porous and shows a fractal nature[49,56,57] as can be seen by using electron microscopy (Figure 1a). A low-resolution top surface SEM confirms (Figure 1a) the formation of porous silicon in wire-like structure formed as a consequence of reaction between the Si wafer and the etching solution (eqs R1−R3, Supporting Information). To noticeably see the nanoporous fractal structures, TEM has been performed, and sizes from a wire-like portion (from square box) have been qualitatively estimated. The presence of wire-like structures has been clearly confirmed along with the formation of embedded nanostructures of size ~5 nm, as apparent from the magnified TEM image on the top right side (lateral-right inset, Figure 1a). It is important to mention here that not much variation in the diameter of the Si wire can be noticed at the macroscopic level. To quantify the nanometer size, Raman spectroscopy has been performed on the sample which shows a red-shifted and asymmetrically broadened Raman spectrum (green curve, Figure 1b). In the confined systems, the behavior of restricted phonons is governed by an asymmetric Raman line shape deviating from its bulk counterpart due to the relaxation in momentum conservation. An appropriate Raman line shape accounting for phonon confinement was developed by Richter et al.[58] and later modified by Campbell and Fauchet.[59] Various line shapes according to the regimes of suitability have later been developed, accounting for corresponding effects from very small sized nanoclusters,[60,61] amorphous materials,[23,62] and nanocrystals.[63] For the confined interferons,[64,65] participating in electron−phonon interaction,[34,46,66] the porosified sample shows a Raman spectrum with a 13 cm^{-1} broad peak

https://dx.doi.org/10.1021/acs.jpclett.1c00217
J. Phys. Chem. Lett. 2021, 12, 2044−2051

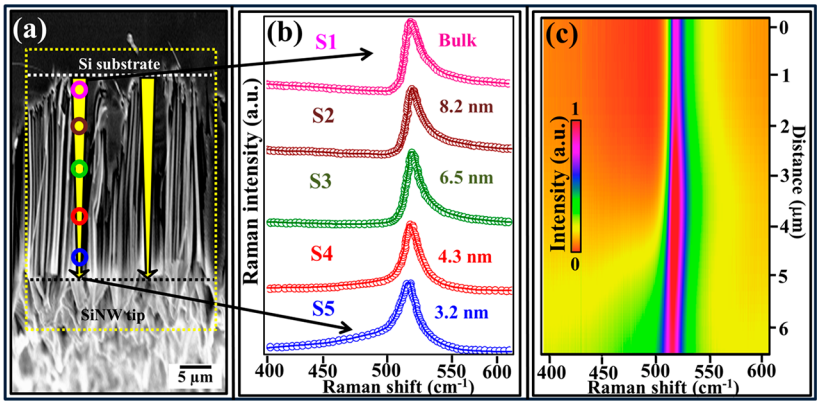

Figure 2. (a) Cross-sectional SEM image of Si wire sample, (b) position-dependent Raman spectra at five different positions along the wire cross section, and (c) the consolidated cross-sectional spatial Raman image generated by using all the Raman spectra acquired during mapping. The position on the *Y*-axis has been marked with respect to the Si substrate. Adapted with permission from ref 66.

centered at 518 cm^{-1} with an asymmetry ratio ($\alpha_r = \gamma_l/\gamma_h$) of 0.8, where γ_l and γ_h are the half-widths toward the lower- and higher-energy sides, respectively, of the spectral maximum. In comparison, the c-Si wafer (used for etching) shows an asymmetric Raman line shape with α_r = 0.4 (brown curve, Figure 1b), meaning a more asymmetric line shape as compared to the Si NSs. The laser-related effects are absent, and being a nonpolar semiconductor, the role of surface phonons is also ruled out.[67−70] Thus, the relaxation in asymmetry, consequent to reduction in size, takes place due to confined interferons in the Si NSs, and accordingly the Raman line shapes are analyzed by using the line shape function predicted by the Fantum model[71] (more details in the Supporting Information) given by eq 1 to quantify the size and Fano parameter, q

$$I(\omega, L) = \int_0^1 \exp\left\{-\frac{k^2L^2}{4a^2}\right\}\frac{(\varepsilon + q)^2}{1 + \varepsilon^2}\,\mathrm{k.dk} \tag{1}$$

Here $\varepsilon = \frac{\omega - \omega(k)}{\Gamma/2}$ and L, and Γ denote the nanocrystallite size, lattice constant, and line width (4 cm^{-1}) of c-Si, respectively. $\omega(k) = \sqrt{171400 + 100000\cos\frac{\pi k}{2}}$ is the phonon dispersion relation for Si and q is the Fano asymmetry parameter which is a measure of the extent of electron−phonon interaction present in the system. As mentioned above, the overlapping of electronic energy with a discrete phonon gives rise to an asymmetric line shape due to interference.[45,72,73] Such Raman line shapes have two distinct features: First, the doping-dependent asymmetry in the Fano−Raman line shape should be broader on the lower energy side of the peak for an n-type semiconductor ($\alpha_r > 1$), whereas it should be broader on the high energy side of the peak for a p-type semiconductor ($\alpha_r < 1$).[45] Second, the signature of the presence of the Fano effect in a system is the observation of antiresonance. The antiresonance and broadening of half-widths are observed on opposite sides of the peak in the spectrum showing Fano interaction. This model predicts an asymmetric Raman line shape which can be fitted with the experimental Raman data to estimate the Si NSs size and q for further analysis and to deconvolute the individual effects, namely the e-phonon interaction and quantum confinement. The corresponding fitting of Raman data in Figure 1b with eq 1 yields q values of 4 and 10 from c-Si and an average size of 6 nm of the Si NSs, respectively, which is consistent with the experimentally observed asymmetry and width (full width at half-maximum, or FWHM) mentioned above. It is important here to mention that a larger value of q (= 10) is obtained from Si NSs as compared to that (q = 4) for c-Si, indicating a stronger Fano interaction in the latter. This is not consistent with the well-known size-dependent Fano effect,[33,73,74] which predicts a strong Fano coupling in smaller Si NSs. To discount, or confirm, a possible anomaly in the size dependence of interferons' behavior, further investigations are required and accordingly understood. Raman spectroscopy, an established tool with advantages over several other techniques,[13,75] has been used here to investigate the above-mentioned anomaly in the size-dependent interferon behavior as discussed below.

The fractal-like geometry of nanostructures and the fabrication techniques invite a preferentially advanced investigation using Raman spectroscopy to uncover anomalies that are concealed in the explicit manifestation of quantum confinement. Top surface Raman spectra are expected to have information about the size only from (and near) the tip of the nanowire, henceforth not delivering complete information about whole sample, and thus various phenomena that require an overall assessment of system remain untouched. To understand the true nature of various subtle processes, cross-sectional Raman spectromicroscopy of a porosified sample has been done by obtaining Raman spectra along the length of the wire starting from substrate (c-Si) to the tip of nanowire, as shown in the SEM image in Figure 2a. Raman spectra obtained from five different positions along the wire are shown in Figure 2b (the legends have been marked to guide the location from where spectra have been recorded). The experimental Raman data (discrete points) have been theoretically fitted by using the FANTUM[54,73,74] line shape function (eq 1) which gives information about the confined interferons rather than only phonons. The Si NSs' size and Fano parameter, obtained corresponding to best fitting (solid line, Figure 2b), are listed in Table 1. The five Raman spectra used for the size-dependent study are only representative data out of several Raman spectra recorded to study the longitudinal variation in the Raman spectral feature as can be seen in the form of the Raman image (Figure 2c). The Raman image in Figure 2c clearly shows how the Raman spectra vary along the length of the wire and how the line shape changes from a value of $\alpha_r < 1$ to $\alpha_r > 1$ while scanning from the substrate to the tip of the wire. Such variation along the length of the Si wire is attributed due to the

https://dx.doi.org/10.1021/acs.jpclett.1c00217
J. Phys. Chem. Lett. 2021, 12, 2044−2051

Table 1. Estimated Fano Parameters (q) and Si NSs Size (L) Obtained from Theoretical Fitting (Using Eq 1) of Different Raman Spectra in Figure 2b

longitudinal position (Figure 2)	S1	S2	S3	S4	S5
q	4	6.4	7.3	8.5	10
L (nm)	∞ (bulk)	8.2	6.5	4.3	3.2

longitudinal variation in Si NSs size as a consequence of the fractal nature of the sample[66] introduced due to the etching process.

The estimated Si NSs size and the analysis of Fano parameters (Table 1) show clearly that the Si NSs size decreases along the wire from the substrate (point S1, bulk) to the tip of the nanowire (point S5, 3.2 nm). Along with the variation of size across the wire, it is also important to note the variation of q which depicts the strength of electron−phonon interaction in these sizes. As reported by Sagar et al.[33] and Kumar et al.,[34] increased quantum confinement (smaller NSs size) leads to a stronger electron−phonon interaction, which on the contrary in this case is increasing, as evident from theoretical fitting using the FANTUM model (Supporting Information) and Table 1. The apparent anomaly in Figure 1 appears evident (Figure 2b and Table 1) from the ambiguous set of obtained parameters indicating the anomalous interaction of quantum confined interferons. Also, before attempting to explain this anomaly, it is important to mention here that the reported quantum "$q-L$" variation is valid for a given doping (carrier) concentrations in the sample.[34,76] In other words, the above-mentioned behavior can be said to be anomalous only if the dopant concentration (an important parameter in the Fano interaction) remains constant along the Si wire. In contrast, a possibility of reduction in carrier concentration due to dopants' migration has been predicted[48] which means that a continuous variation of carrier concentration along the whole length is possible. In other words, the sample doping reduces as one move from substrate to the tip of wire due to migration of dopant atoms along with reduction in nanostructure sizes.

The above-mentioned hypothesis, to be validated later on, has been explained by considering the Si NSs size variation along the wire's length to be graded rather than continuous for easier modeling. Figure 3 shows a schematic diagram depicting the combined effect of band gap enhancement and dopant mass migration as the size of the microscopic nanostructures gets reduced (bulk to L4), where the latter is supposed to be a consequence of fabrication technique involved for the porosification of the sample. As is apparent from q values estimated for different sizes, the anomalous decrease of electron−phonon interaction with decreasing size is discernible in the whole picture (Table 1). But a microscopic assessment leads to two different phenomena, namely, quantum confinement and mass migration of dopant atoms; decoding this anomaly proves it to be a pseudo-paradox.

Interplay between these two is known to cause such an anomaly and thus falsifying the actual picture at the macroscopic level which can be validated as follows. The band gap enhancement due to quantum confinement is a noted phenomenon[32] leading to increase in band gap, visible on the same sample in the present case as one moves from the substrate (c-Si) to the tip of SiNWs. A constant Fermi level, being representative of the whole sample, predicts that different regions along the wire length consist of different

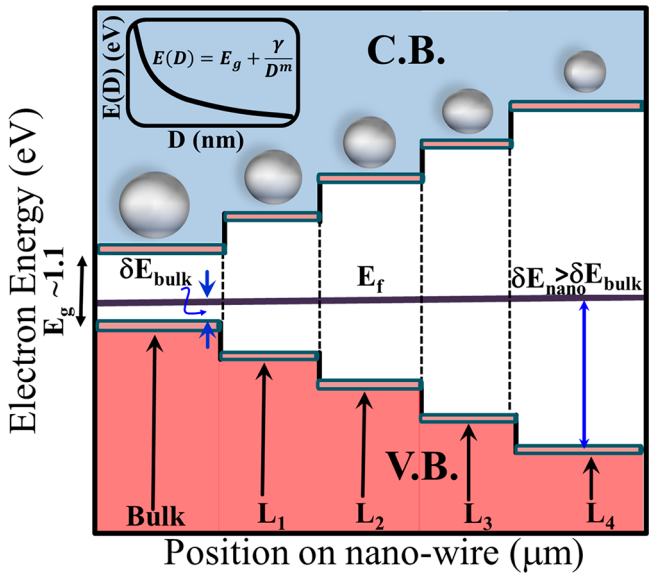

Figure 3. Schematic representation of combined effect dopants' mass migration and quantum confinement on the band structure of fractal Si wire where the relative position of intrinsic and heavily doped p-type wafer has been marked with dotted and solid lines, respectively, along with the inset showing the typical band gap vs size variation.

carrier concentrations as can be recognized from its position relative to the band edge.[48] It is clear from Figure 3 that the dopant's concentration is minimum in the region on the wire where the smallest Si NSs are present. Because the Fano coupling is directly proportional to the carrier concentration,[76] a poor Fano coupling between the thus-generated continuum and confined phonon will become inevitable near the tip of the wire. At the same time, the quantum size effect will be maximum at the tip, thus enforcing a stronger coupling. On the whole, the dominating of the two effects will dictate the overall Raman line shape. In the current scenario it appears that the Fano component is eventually small near the tip where Si NSs are the smallest. Before one makes the final conclusions about the most dominant cause, a better clarity about the available size-dependent dopants' concentration, at last some quantification is necessary.

The above-mentioned depletion of dopants (boron in this case) can be semiquantified directly by using the analysis of the boron peak in the Raman spectra recorded from different positions along the wire's length (Figure 4a). Plenty of boron ions are present in the substrate, as evident from a clear peak near 620 cm^{-1} (pink curve) originating from borons[77] present in the Si lattice. The intensity of this peak continuously decreases while moving toward the surface of the sample. The intensity of this peak completely vanishes in the Raman spectrum collected from the tip (surface) region, meaning that few borons are present near the surface. The concentration of the boron atoms is actually inadequate to create sufficient continuum for the Fano interaction to take place. This has been experimentally proven by analyzing the zoomed-in position-dependent Raman spectra (near the base of the spectra), as shown in Figure 4b. The Raman spectra obtained from the substrate region (pink curve) show a clear antiresonance dip, meaning a stronger Fano coupling. The antiresonance dip gradually decreases and vanishes completely in the Raman spectrum collected from the surface region (blue curve) where the Raman spectrum is fully dominated by the

https://dx.doi.org/10.1021/acs.jpclett.1c00217
J. Phys. Chem. Lett. 2021, 12, 2044−2051

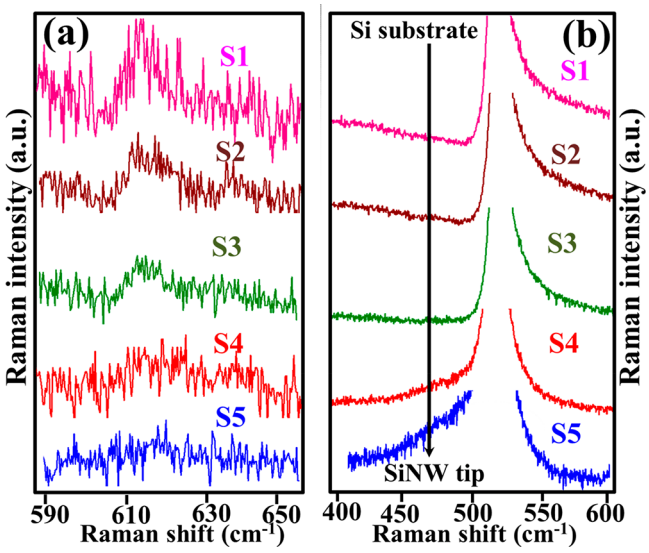

Figure 4. (a) Position-dependent Raman spectra corresponding to localized boron peak (at 620 cm $^{-1}$). (b) Zoomed-in Raman spectra showing decreasing antiresonance while moving from the substrate toward the surface region.

confinement effect. In other words, the available quantum confinement effect is maximum near the surface region (where smallest NSs are present) and makes the phonon confinement effect more dominating as compared to the Fano interaction.

While moving on the Si wire from bulk toward the surface, the decreasing Fano effect recedes to the increasing quantum size effect more rapidly to get overwhelmed by the confinement effect. As mentioned above, a detailed analysis to understand the observed Fano paradox (the anomalous size-dependent variation of the Fano parameter and its interplay with Si NSs size), duly validated by experimental and theoretical approaches, has been presented. A careful analysis of the Raman spectral line shape must be performed without which it may lead to wrong conclusions.

In conclusion, a spatial Raman spectromicroscopic study reveals that confined interferons in silicon (Si) nanostructures (NSs) show a paradoxical variation of the Fano asymmetry parameter (q) with respect to NSs size as compared to the typical quantum confined effect. A detailed theoretical and experimental Raman line shape analysis resolves the anomaly in the reported size vs q dependence. The above-mentioned pseudo-anomalous behavior of interferons, or the "quantum Fano paradox", was found to be a consequence of fractal nature of the Si wires present in the sample which consists of SiNSs of different sizes along the Si wire prepared by metal-assisted etching as clearly seen by using cross-sectional Raman microscopy. The longitudinal variation in Si microcrystallite size (in the nanometer range) actually evokes a gradual depletion of dopants resulting in their etching-induced migration, stronger for smaller nanocrystallites, which recedes to the size-dependent Fano parameter variation. In other words, little Fano coupling in smaller Si NSs is a consequence of lower dopants' concentration rather than the quantum size effect. Besides theoretical Raman line shape deconvolution, the gradual zonal dopants' variation has been experimentally validated by using the analysis of boron's Raman signal variation and associated antiresonance along the Si wire.

■ ASSOCIATED CONTENT

Supporting Information

The Supporting Information is available free of charge at https://pubs.acs.org/doi/10.1021/acs.jpclett.1c00217.

Chemical reaction involved in chemical etching; explanation of Fantum model; Stokes−anti-Stokes Raman spectrum for temperature estimation (PDF)

■ AUTHOR INFORMATION

Corresponding Authors

Ashutosh Sharma − *Department of Materials Science and Engineering, Ajou University, Suwon 16499, Korea*; Email: ashu@ajou.ac.kr

Byungmin Ahn − *Department of Materials Science and Engineering and Department of Energy Systems Research, Ajou University, Suwon 16499, Korea*; orcid.org/0000-0002-0866-6398; Email: byungmin@ajou.ac.kr

Sangyeob Lee − *Department of Materials Science and Engineering, Hanbat National University, Daejeon 34158, Korea*; orcid.org/0000-0002-9957-990X; Email: sangyeob@hanbat.ac.kr

Rajesh Kumar − *Materials and Device Laboratory, Discipline of Physics and Centre for Advanced Electronics, Indian Institute of Technology Indore, Simrol 453552, India*; orcid.org/0000-0001-7977-986X; Email: rajeshkumar@iiti.ac.in

Authors

Manushree Tanwar − *Materials and Device Laboratory, Discipline of Physics, Indian Institute of Technology Indore, Simrol 453552, India*; orcid.org/0000-0002-7589-0496

Devesh K. Pathak − *Materials and Device Laboratory, Discipline of Physics, Indian Institute of Technology Indore, Simrol 453552, India*

Anjali Chaudhary − *Materials and Device Laboratory, Discipline of Physics, Indian Institute of Technology Indore, Simrol 453552, India*; orcid.org/0000-0002-8202-2697

Alexander S. Krylov − *Kirensky Institute of Physics, Federal Research Center KSC SB RAS, Krasnoyarsk 660036, Russia*; orcid.org/0000-0001-8949-0584

Herbert Pfnür − *Institut für Festkörperphysik, Leibniz Universität Hannover, D-30167 Hannover, Germany*; orcid.org/0000-0003-1568-4209

Complete contact information is available at: https://pubs.acs.org/10.1021/acs.jpclett.1c00217

Notes

The authors declare no competing financial interest.

■ ACKNOWLEDGMENTS

The authors acknowledge the Sophisticated Instrumentation Centre (SIC), IIT Indore, for SEM measurements. The authors are thankful for the funding received from Science and Engineering Research Board (SERB), Govt. of India (Grant CRG/2019/000371). Facilities received from the Department of Science and Technology (DST), Govt. of India, under the FIST scheme Grant SR/FST/PSI-225/2016 is highly acknowledged. D.K.P. acknowledges the Council of Scientific and Industrial Research (CSIR) for financial support (file 09/1022(0039)/2017-EMR-I), and M.T. acknowledges DST, Govt. of India, for providing funding (file DST/INSPIRE/03/2018/000910/IF180398). This work was supported by the

https://dx.doi.org/10.1021/acs.jpclett.1c00217
J. Phys. Chem. Lett. 2021, 12, 2044−2051

National Research Foundation of Korea (grant no. 2020R1A4A4079397). The authors thank Dr. Puspen Mondal (RRCAT,Indore) for TEM measurements. Useful discussions with Dr. P. R. Sagdeo (IIT Indore) are also acknowledged.

REFERENCES

(1) Hartsfield, T.; Chang, W.-S.; Yang, S.-C.; Ma, T.; Shi, J.; Sun, L.; Shvets, G.; Link, S.; Li, X. Single Quantum Dot Controls a Plasmonic Cavity's Scattering and Anisotropy. *Proc. Natl. Acad. Sci. U. S. A.* **2015**, *112* (40), 12288−12292.
(2) Ha, S.-T.; Su, R.; Xing, J.; Zhang, Q.; Xiong, Q. Metal Halide Perovskite Nanomaterials: Synthesis and Applications. *Chem. Sci.* **2017**, *8* (4), 2522−2536.
(3) Liu, X.; Pei, J.; Hu, Z.; Zhao, W.; Liu, S.; Amara, M.-R.; Watanabe, K.; Taniguchi, T.; Zhang, H.; Xiong, Q. Manipulating Charge and Energy Transfer between 2D Atomic Layers via Heterostructure Engineering. *Nano Lett.* **2020**, *20* (7), 5359−5366.
(4) Chaudhary, A.; Pathak, D. K.; Tanwar, M.; Yogi, P.; Sagdeo, P. R.; Kumar, R. Polythiophene−PCBM-Based All-Organic Electrochromic Device: Fast and Flexible. *ACS Appl. Electron. Mater.* **2019**, *1* (1), 58−63.
(5) Chaudhary, A.; Pathak, D. K.; Tanwar, M.; Koch, J.; Pfnür, H.; Kumar, R. Polythiophene-NanoWO3 Bilayer as an Electrochromic Infrared Filter: A Transparent Heat Shield. *J. Mater. Chem. C* **2020**, *8*, 1773.
(6) Pathak, D. K.; Chaudhary, A.; Tanwar, M.; Goutam, U. K.; Kumar, R. Nano-Cobalt Oxide/Viologen Hybrid Solid State Device: Electrochromism beyond Chemical Cell. *Appl. Phys. Lett.* **2020**, *116* (14), 141901.
(7) Chaudhary, A.; Pathak, D. K.; Ghosh, T.; Kandpal, S.; Tanwar, M.; Rani, C.; Kumar, R. Prussian Blue-Cobalt Oxide Double Layer for Efficient All-Inorganic Multicolor Electrochromic Device. *ACS Appl. Electron. Mater.* **2020**, *2* (6), 1768−1773.
(8) Zhang, K.; Wei, Y.; Zhang, J.; Ma, H.; Yang, X.; Lu, G.; Zhang, K.; Li, Q.; Jiang, K.; Fan, S. Electrical Control of Spatial Resolution in Mixed-Dimensional Heterostructured Photodetectors. *Proc. Natl. Acad. Sci. U. S. A.* **2019**, *116* (14), 6586−6593.
(9) Leaw, J. N.; Tang, H.-K.; Trushin, M.; Assaad, F. F.; Adam, S. Universal Fermi-Surface Anisotropy Renormalization for Interacting Dirac Fermions with Long-Range Interactions. *Proc. Natl. Acad. Sci. U. S. A.* **2019**, *116* (52), 26431−26434.
(10) Pathak, D. K.; Chaudhary, A.; Tanwar, M.; Goutam, U. K.; Mondal, P.; Kumar, R. Nickel Cobalt Oxide Nanoneedles for Electrochromic Glucose. *ACS Appl. Nano Mater.* **2021**, DOI: 10.1021/acsanm.0c03451.
(11) Driza, N.; Blanco-Canosa, S.; Bakr, M.; Soltan, S.; Khalid, M.; Mustafa, L.; Kawashima, K.; Christiani, G.; Habermeier, H.-U.; Khaliullin, G.; Ulrich, C.; Le Tacon, M.; Keimer, B. Long-Range Transfer of Electron−Phonon Coupling in Oxide Superlattices. *Nat. Mater.* **2012**, *11* (8), 675−681.
(12) Matthews, O. A.; Shipway, A. N.; Stoddart, J. F. Dendrimers—Branching out from Curiosities into New Technologies. *Prog. Polym. Sci.* **1998**, *23* (1), 1−56.
(13) Yogi, P.; Mishra, S.; Saxena, S. K.; Kumar, V.; Kumar, R. Fano Scattering: Manifestation of Acoustic Phonons at the Nanoscale. *J. Phys. Chem. Lett.* **2016**, *7* (24), 5291−5296.
(14) Kroner, M.; Govorov, A. O.; Remi, S.; Biedermann, B.; Seidl, S.; Badolato, A.; Petroff, P. M.; Zhang, W.; Barbour, R.; Gerardot, B. D.; Warburton, R. J.; Karrai, K. The Nonlinear Fano Effect. *Nature* **2008**, *451* (7176), 311−314.
(15) Krylov, A. S.; Sofronova, S. N.; Gudim, I. A.; Krylova, S. N.; Kumar, R.; Vtyurin, A. N. Manifestation of Magnetoelastic Interactions in Raman Spectra of HoxNd1−xFe3(BO3)4 Crystals. *J. Adv. Dielectr.* **2018**, *08* (02), 1850011.
(16) Sharma, M.; Rani, S.; Pathak, D. K.; Bhatia, R.; Kumar, R.; Sameera, I. Manifestation of Anharmonicities in Terms of Phonon Modes' Energy and Lifetime in Multiwall Carbon Nanotubes. *Carbon* **2021**, *171*, 568−574.
(17) Shukla, A. K.; Kumar, R.; Kumar, V. Electronic Raman Scattering in the Laser-Etched Silicon Nanostructures. *J. Appl. Phys.* **2010**, *107* (1), 014306.
(18) Mishra, S.; Yogi, P.; Saxena, S. K.; Roy, S.; Sagdeo, P. R.; Kumar, R. Fast Electrochromic Display: Tetrathiafulvalene−Graphene Nanoflake as Facilitating Materials. *J. Mater. Chem. C* **2017**, *5* (36), 9504−9512.
(19) Gruson, V.; Barreau, L.; Jiménez-Galan, Á.; Risoud, F.; Caillat, J.; Maquet, A.; Carré, B.; Lepetit, F.; Hergott, J.-F.; Ruchon, T.; Argenti, L.; Taïeb, R.; Martín, F.; Salières, P. Attosecond Dynamics through a Fano Resonance: Monitoring the Birth of a Photoelectron. *Science* **2016**, *354* (6313), 734−738.
(20) Ott, C.; Kaldun, A.; Raith, P.; Meyer, K.; Laux, M.; Evers, J.; Keitel, C. H.; Greene, C. H.; Pfeifer, T. Lorentz Meets Fano in Spectral Line Shapes: A Universal Phase and Its Laser Control. *Science* **2013**, *340* (6133), 716−720.
(21) Prusty, S.; Mavi, H. S.; Shukla, A. K. Optical Nonlinearity in Silicon Nanoparticles: Effect of Size and Probing Intensity. *Phys. Rev. B: Condens. Matter Mater. Phys.* **2005**, *71* (11), 113313.
(22) Wang, K.; De Greve, K.; Jauregui, L. A.; Sushko, A.; High, A.; Zhou, Y.; Scuri, G.; Taniguchi, T.; Watanabe, K.; Lukin, M. D.; Park, H.; Kim, P. Electrical Control of Charged Carriers and Excitons in Atomically Thin Materials. *Nat. Nanotechnol.* **2018**, *13* (2), 128−132.
(23) Yogi, P.; Tanwar, M.; Saxena, S. K.; Mishra, S.; Pathak, D. K.; Chaudhary, A.; Sagdeo, P. R.; Kumar, R. Quantifying the Short-Range Order in Amorphous Silicon by Raman Scattering. *Anal. Chem.* **2018**, *90* (13), 8123−8129.
(24) Abidi, D.; Jusserand, B.; Fave, J.-L. Raman Scattering Studies of Heavily Doped Microcrystalline Porous Silicon and Porous Silicon Free-Standing Membranes. *Phys. Rev. B: Condens. Matter Mater. Phys.* **2010**, *82* (7), 075210.
(25) Fano, U. Effects of Configuration Interaction on Intensities and Phase Shifts. *Phys. Rev.* **1961**, *124* (6), 1866−1878.
(26) Bar-Ad, S.; Kner, P.; Marquezini, M. V.; Mukamel, S.; Chemla, D. S. Quantum Confined Fano Interference. *Phys. Rev. Lett.* **1997**, *78* (7), 1363−1366.
(27) Bell, M. J. V.; Ioriatti, L.; Nunes, L. A. O. Fano Interference in Periodic GaAs Doping Multilayers. *Phys. Rev. B: Condens. Matter Mater. Phys.* **1998**, *57* (24), R15104−R15107.
(28) Gupta, R.; Xiong, Q.; Adu, C. K.; Kim, U. J.; Eklund, P. C. Laser-Induced Fano Resonance Scattering in Silicon Nanowires. *Nano Lett.* **2003**, *3* (5), 627−631.
(29) Brongersma, M. L.; Kik, P. G.; Polman, A.; Min, K. S.; Atwater, H. A. Size-Dependent Electron-Hole Exchange Interaction in Si Nanocrystals. *Appl. Phys. Lett.* **2000**, *76* (3), 351−353.
(30) Spanier, J. E.; Robinson, R. D.; Zhang, F.; Chan, S.-W.; Herman, I. P. Size-Dependent Properties of CeO_{2-Y} Nanoparticles as Studied by Raman Scattering. *Phys. Rev. B: Condens. Matter Mater. Phys.* **2001**, DOI: 10.1103/PhysRevB.64.245407.
(31) Saxena, K.; Kumar, V.; Shukla, A. K. Size-Dependent Photoluminescence in Silicon Nanostructures: Quantum Confinement Effect. *Micro Nano Lett.* **2013**, *8* (6), 311−314.
(32) Collins, R. T.; Fauchet, P. M.; Tischler, M. A. Porous Silicon: From Luminescence to LEDs. *Phys. Today* **1997**, *50* (1), 24−31.
(33) Sagar, D. M.; Atkin, J. M.; Palomaki, P. K. B.; Neale, N. R.; Blackburn, J. L.; Johnson, J. C.; Nozik, A. J.; Raschke, M. B.; Beard, M. C. Quantum Confined Electron−Phonon Interaction in Silicon Nanocrystals. *Nano Lett.* **2015**, *15* (3), 1511−1516.
(34) Kumar, R.; Shukla, A.; Mavi, H.; Vankar, V. Size-Dependent Fano Interaction in the Laser-Etched Silicon Nanostructures. *Nanoscale Res. Lett.* **2008**, *3* (3), 105.
(35) Ray, S. C.; Low, Y.; Tsai, H. M.; Pao, C. W.; Chiou, J. W.; Yang, S. C.; Chien, F. Z.; Pong, W. F.; Tsai, M.-H.; Lin, K. F.; Cheng, H. M.; Hsieh, W. F.; Lee, J. F. Size Dependence of the Electronic Structures and Electron-Phonon Coupling in ZnO Quantum Dots. *Appl. Phys. Lett.* **2007**, *91* (26), 262101.
(36) Lin, C.; Gong, K.; Kelley, D. F.; Kelley, A. M. Size-Dependent Exciton−Phonon Coupling in CdSe Nanocrystals through Resonance

Raman Excitation Profile Analysis. *J. Phys. Chem. C* **2015**, *119* (13), 7491−7498.
(37) Raman, C. V.; Krishnan, K. S. A New Type of Secondary Radiation. *Nature* **1928**, *121* (3048), 501−502.
(38) Raman, C. A New Radiation. *Indian J. Phys.* **1928**, *02*, 387−398.
(39) Kumar, R. Asymmetry to Symmetry Transition of Fano Line-Shape: Analytical Description. *Indian J. Phys.* **2013**, *87* (1), 49−52.
(40) Piscanec, S.; Cantoro, M.; Ferrari, A. C.; Zapien, J. A.; Lifshitz, Y.; Lee, S. T.; Hofmann, S.; Robertson, J. Raman Spectroscopy of Silicon Nanowires. *Phys. Rev. B: Condens. Matter Mater. Phys.* **2003**, *68* (24), 241312.
(41) Cerdeira, F.; Cardona, M. Effect of Carrier Concentration on the Raman Frequencies of Si and Ge. *Phys. Rev. B* **1972**, *5* (4), 1440−1454.
(42) Cerdeira, F.; Fjeldly, T. A.; Cardona, M. Interaction between Electronic and Vibronic Raman Scattering in Heavily Doped Silicon. *Solid State Commun.* **1973**, *13* (3), 325−328.
(43) Magidson, V.; Beserman, R. Fano-Type Interference in the Raman Spectrum of Photoexcited Si. *Phys. Rev. B: Condens. Matter Mater. Phys.* **2002**, *66* (19), 195206.
(44) Chandrasekhar, M.; Renucci, J. B.; Cardona, M. Effects of Interband Excitations on Raman Phonons in Heavily Doped N-Si. *Phys. Rev. B: Condens. Matter Mater. Phys.* **1978**, *17* (4), 1623−1633.
(45) Saxena, S. K.; Yogi, P.; Mishra, S.; Rai, H. M.; Mishra, V.; Warshi, M. K.; Roy, S.; Mondal, P.; Sagdeo, P. R.; Kumar, R. Amplification or Cancellation of Fano Resonance and Quantum Confinement Induced Asymmetries in Raman Line-Shapes. *Phys. Chem. Chem. Phys.* **2017**, *19* (47), 31788−31795.
(46) Kumar, R.; Mavi, H. S.; Shukla, A. K.; Vankar, V. D. Photoexcited Fano Interaction in Laser-Etched Silicon Nanostructures. *J. Appl. Phys.* **2007**, *101* (6), 064315.
(47) Nychyporuk, T.; Lysenko, V.; Barbier, D. Fractal Nature of Porous Silicon Nanocrystallites. *Phys. Rev. B: Condens. Matter Mater. Phys.* **2005**, *71* (11), 115402.
(48) Tanwar, M.; Pathak, D. K.; Chaudhary, A.; Saxena, S. K.; Kumar, R. Unintended Deviation of Fermi Level from Band Edge in Fractal Silicon Nanostructures: Consequence of Dopants' Zonal Depletion. *J. Phys. Chem. C* **2020**, *124* (30), 16675−16679.
(49) Yogi, P.; Saxena, S. K.; Chaudhary, A.; Pathak, D. K.; Mishra, S.; Mondal, P.; Joshi, B.; Sagdeo, P. R.; Kumar, R. Porous Silicon's Fractal Nature Revisited. *Superlattices Microstruct.* **2018**, *120*, 141−147.
(50) Huang, Z.; Geyer, N.; Werner, P.; de Boor, J.; Gösele, U. Metal-Assisted Chemical Etching of Silicon: A Review. *Adv. Mater.* **2011**, *23* (2), 285−308.
(51) Chern, W.; Hsu, K.; Chun, I. S.; Azeredo, B. P. de; Ahmed, N.; Kim, K.-H.; Zuo, J.; Fang, N.; Ferreira, P.; Li, X. Nonlithographic Patterning and Metal-Assisted Chemical Etching for Manufacturing of Tunable Light-Emitting Silicon Nanowire Arrays. *Nano Lett.* **2010**, *10* (5), 1582−1588.
(52) Chartier, C.; Bastide, S.; Lévy-Clément, C. Metal-Assisted Chemical Etching of Silicon in HF−H_2O2. *Electrochim. Acta* **2008**, *53* (17), 5509−5516.
(53) Saxena, S. K.; Kumar, V.; Rai, H. M.; Sahu, G.; Late, R.; Saxena, K.; Shukla, A. K.; Sagdeo, P. R.; Kumar, R. Study of Porous Silicon Prepared Using Metal-Induced Etching (MIE): A Comparison with Laser-Induced Etching (LIE). *Silicon* **2017**, *9* (4), 483−488.
(54) Tanwar, M.; Chaudhary, A.; Pathak, D. K.; Yogi, P.; Saxena, S. K.; Sagdeo, P. R.; Kumar, R. Deconvoluting Diffuse Reflectance Spectra for Retrieving Nanostructures' Size Details: An Easy and Efficient Approach. *J. Phys. Chem. A* **2019**, *123* (16), 3607−3614.
(55) Neeshu, K.; Rani, C.; Kaushik, R.; Tanwar, M.; Pathak, D.; Chaudhary, A.; Kumar, A.; Kumar, R. Size Dependence of Raman Line-Shape Parameters Due to Confined Phonons in Silicon Nanowires. *Adv. Mater. Process. Technol.* **2020**, *6* (0), 669−676.
(56) Saxena, S. K.; Yogi, P.; Yadav, P.; Mishra, S.; Pandey, H.; Rai, H. M.; Kumar, V.; Sagdeo, P. R.; Kumar, R. Role of Metal Nanoparticles on Porosification of Silicon by Metal Induced Etching (MIE). *Superlattices Microstruct.* **2016**, *94*, 101−107.
(57) Yogi, P.; Poonia, D.; Yadav, P.; Mishra, S.; Saxena, S. K.; Roy, S.; Sagdeo, P. R.; Kumar, R. Tent-Shaped Surface Morphologies of Silicon: Texturization by Metal Induced Etching. *Silicon* **2018**, *10* (6), 2801−2807.
(58) Richter, H.; Wang, Z. P.; Ley, L. The One Phonon Raman Spectrum in Microcrystalline Silicon. *Solid State Commun.* **1981**, *39* (5), 625−629.
(59) Campbell, I. H.; Fauchet, P. M. The Effects of Microcrystal Size and Shape on the One Phonon Raman Spectra of Crystalline Semiconductors. *Solid State Commun.* **1986**, *58* (10), 739−741.
(60) Koniakhin, S. V.; Utesov, O. I.; Terterov, I. N.; Siklitskaya, A. V.; Yashenkin, A. G.; Solnyshkov, D. Raman Spectra of Crystalline Nanoparticles: Replacement for the Phonon Confinement Model. *J. Phys. Chem. C* **2018**, *122* (33), 19219−19229.
(61) Koniakhin, S. V.; Utesov, O. I.; Yashenkin, A. G. Lifetimes of Confined Optical Phonons and the Shape of a Raman Peak in Disordered Nanoparticles. II. Numerical Treatment. *Phys. Rev. B: Condens. Matter Mater. Phys.* **2020**, *102* (20), 205422.
(62) Tanwar, M.; Yogi, P.; Lambora, S.; Mishra, S.; Saxena, S. K.; Sagdeo, P. R.; Krylov, A. S.; Kumar, R. Generalisation of Phonon Confinement Model for Interpretation of Raman Line-Shape from Nano-Silicon. *Adv. Mater. Process. Technol.* **2018**, *4* (2), 227−233.
(63) Faraci, G.; Gibilisco, S.; Russo, P.; Pennisi, A. R.; La Rosa, S. Modified Raman Confinement Model for Si Nanocrystals. *Phys. Rev. B: Condens. Matter Mater. Phys.* **2006**, *73* (3), 033307.
(64) Kumar, R.; Shukla, A. K. Quantum Interference in the Raman Scattering from the Silicon Nanostructures. *Phys. Lett. A* **2009**, *373* (32), 2882−2886.
(65) Sahu, G.; Kumar, R.; Mahapatra, D. P. Raman Scattering and Backscattering Studies of Silicon Nanocrystals Formed Using Sequential Ion Implantation. *Silicon* **2014**, *6* (1), 65−71.
(66) Tanwar, M.; Pathak, D. K.; Chaudhary, A.; Yogi, P.; Saxena, S. K.; Kumar, R. Mapping Longitudinal Inhomogeneity in Nanostructures Using Cross-Sectional Spatial Raman Imaging. *J. Phys. Chem. C* **2020**, *124* (11), 6467−6471.
(67) Adu, K. W.; Xiong, Q.; Gutierrez, H. R.; Chen, G.; Eklund, P. C. Raman Scattering as a Probe of Phonon Confinement and Surface Optical Modes in Semiconducting Nanowires. *Appl. Phys. A: Mater. Sci. Process.* **2006**, *85* (3), 287.
(68) Mahan, G. D.; Gupta, R.; Xiong, Q.; Adu, C. K.; Eklund, P. C. Optical Phonons in Polar Semiconductor Nanowires. *Phys. Rev. B: Condens. Matter Mater. Phys.* **2003**, *68* (7), 073402.
(69) Begum, N.; Bhatti, A. S.; Jabeen, F.; Rubini, S.; Martelli, F. Lineshape Analysis of Raman Scattering from LO and SO Phonons in III-V Nanowires. *J. Appl. Phys.* **2009**, *106* (11), 114317.
(70) Gupta, R.; Xiong, Q.; Mahan, G. D.; Eklund, P. C. Surface Optical Phonons in Gallium Phosphide Nanowires. *Nano Lett.* **2003**, *3* (12), 1745−1750.
(71) Yogi, P.; Poonia, D.; Mishra, S.; Saxena, S. K.; Roy, S.; Kumar, V.; Sagdeo, P. R.; Kumar, R. Spectral Anomaly in Raman Scattering from P-Type Silicon Nanowires. *J. Phys. Chem. C* **2017**, *121* (9), 5372−5378.
(72) Burke, B. G.; Chan, J.; Williams, K. A.; Wu, Z.; Puretzky, A. A.; Geohegan, D. B. Raman Study of Fano Interference in P-Type Doped Silicon. *J. Raman Spectrosc.* **2010**, *41* (12), 1759−1764.
(73) Saxena, S. K.; Borah, R.; Kumar, V.; Rai, H. M.; Late, R.; Sathe, V. G.; Kumar, A.; Sagdeo, P. R.; Kumar, R. Raman Spectroscopy for Study of Interplay between Phonon Confinement and Fano Effect in Silicon Nanowires. *J. Raman Spectrosc.* **2016**, *47* (3), 283−288.
(74) Yogi, P.; Saxena, S. K.; Mishra, S.; Rai, H. M.; Late, R.; Kumar, V.; Joshi, B.; Sagdeo, P. R.; Kumar, R. Interplay between Phonon Confinement and Fano Effect on Raman Line Shape for Semiconductor Nanostructures: Analytical Study. *Solid State Commun.* **2016**, *230*, 25−29.
(75) Hessel, C. M.; Wei, J.; Reid, D.; Fujii, H.; Downer, M. C.; Korgel, B. A. Raman Spectroscopy of Oxide-Embedded and Ligand-

https://dx.doi.org/10.1021/acs.jpclett.1c00217
J. Phys. Chem. Lett. 2021, 12, 2044−2051

Stabilized Silicon Nanocrystals. *J. Phys. Chem. Lett.* **2012**, *3* (9), 1089−1093.
(76) Jain, K. P.; Shukla, A. K.; Abbi, S. C.; Balkanski, M. Raman Scattering in Ultraheavily Doped Silicon. *Phys. Rev. B: Condens. Matter Mater. Phys.* **1985**, *32* (8), 5464−5467.
(77) Cerdeira, F.; Fjeldly, T. A.; Cardona, M. Raman Study of the Interaction between Localized Vibrations and Electronic Excitations in Boron-Doped Silicon. *Phys. Rev. B* **1974**, *9* (10), 4344−4350.

https://dx.doi.org/10.1021/acs.jpclett.1c00217
J. Phys. Chem. Lett. 2021, 12, 2044−2051